FLUXMETER FOR POINT-FOCUS SOLAR CONCENTRATORS

A. Parretta*[1], A. Antonini[2], M. Stefancich[2], G. Martinelli[2], M. Armani[3]
[1]ENEA Centro Ricerche "E. Clementel", Via Martiri di Monte Sole 4, 40129 Bologna (BO), Italy.
[2]Physics Dept., University of Ferrara, Via Saragat 1, 44100 Ferrara (FE), Italy.
[3]Institute for Renewable Energy, EURAC reasearch, Viale Druso 1, 39100 Bolzano (BZ), Italy.
*Phone: +39 (0)51 6098617; Fax: +39 (0)51 6098767; E-mail: antonio.parretta@bologna.enea.it

ABSTRACT

A fluxmeter for high flux density measurements in point-focus solar concentrators is based on the use of two integrating spheres, coupled by an intermediate window of selected aperture area. The concentrated radiation is collected by the first sphere through an input window, integrated and driven to the second sphere where it is coupled to a conventional radiometer and to a spectrometer for flux and spectral measurements, respectively. The overall attenuation factor of input radiation is controlled by selecting the area of intermediate window. Attenuation levels from few tens up to few thousands can be well controlled. The fluxmeter has been calibrated by a pulsed solar simulator modified to operate with concentrated radiation at levels of hundreds of suns. An optical model and a ray-tracing study have been also developed and validated, by which the optical and thermal properties of the fluxmeter have been fully explored.

INTRODUCTION

The characterization of the concentrated solar beam is a direct way to perform the optical characterization of a solar concentrator. Among the direct methods, one of the most used is the camera-target one [1, 2], which gives the irradiance profile of the beam on the surface of a Lambertian target. We have theoretically analyzed the camera-target method for planar targets and produced an associated image reconstruction algorithm [3]. For a complete optical characterization of the beam, however, supplementary measurements of the absolute flux density are required, at least on some points of the tested plane, by reference calorimeters [4]. In this paper we present the last results obtained by developing a fluxmeter devoted to point-focus solar concentrators of the Fresnel type, also useful for indoor testing of small concentrator prototypes, easy to operate and portable. The fluxmeter operates under a stationary irradiation regime and the photodetector is thermoregulated to avoid variation of sensitivity at changing irradiation level. The fluxmeter provides also the spectral irradiance distribution of the concentrated radiation.

THE METHOD

Fig. 1 shows the basic scheme of the fluxmeter. The two interconnected optical cavities (is1) and (is2) are obtained by hollowing an Aluminium prism (pr) and operate as integrating spheres. The concentrated radiation (cl) enters the first cavity (is1) through the window (win). Radiation is then transferred to the second cavity (is2) through the intermediate window (wco) which can be varied according to the intensity of the input beam by using one in a series of inserts provided with holes of different area. Cavity (is2) is coupled to the photodetector (pd) for flux measurement by radiometer (rad), and to the optical fiber (of) for spectral measurement by spectrometr (sp). The input window (win) is selected depending on the type of measurement being carried out. It provides the input of the focused beam for total flux measurement, or a portion of the beam for flux density mapping. In the last case the radiometer can be moved in front of the beam by an electronically driven x-y translation stage.

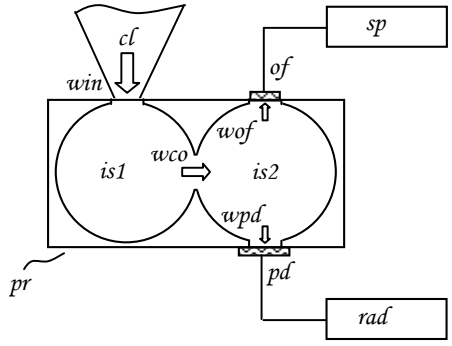

Fig. 1. Schematic of the fluxmeter.

THE OPTICAL MODEL

The fluxmeter has been optically modelled by applying the conservation law for the input flux. The main parameters of the model are: the flux Φ_0 at input window (win) of area S_{in}; the diameter d and the wall reflectance R_w common to both spheres; the aperture area S_{co} of the intermediate window (wco); the flux Φ_m on the photodetector (pd) with area S_m and reflectance R_m; the area S_{of} and reflectance R_{of} of the optical fibre (of) head; the irradiance G_0 at input window (win), the irradiance G_1 on the wall of cavity (is1) and the irradiance G_2 on the wall of cavity (is2). We define also the attenuation factor for flux, f_A^{Φ}, as the ratio between flux Φ_0 at input and flux Φ_m on the photodetector (pd):

$$f_A^{\Phi} = \Phi_0 / \Phi_m \qquad (1)$$

By applying the flux conservation law, we obtain for the attenuation factor for flux:

$$f_A^{\Phi} = S_{in} \cdot G_0 / S_m \cdot G_2 = \frac{\Sigma_1 \cdot \Sigma_2 - S_{co}^{\ 2}}{S_m \cdot S_{co}} \qquad (1')$$

where:

$$\sum\nolimits_1 = [S_{in} + S_{co} + S_{w1} \cdot (1 - R_w)] ;$$

$$\sum\nolimits_2 = [S_m \cdot (1 - R_m) + S_{of} \cdot (1 - R_{of}) + \ldots$$

$$\ldots S_{co} + S_{w2} \cdot (1 - R_w)]$$

and where S_{w1} is the wall surface area in sphere (is1) and S_{w2} the wall surface area in sphere (is2), which are different due to different window openings. The optical model has been tested fixing all parameters except the aperture area S_{co} and the wall reflectance R_w. The fixed parameters were; $S_{in} = S_m$ = 1,21 cm^2; d = 5 cm; S_{of} = 0,2 cm^2; R_m = 4%; R_{of} = 84%. The SunPower HECO252 concentration cell was used as photodetector. Fig. 2 shows the attenuation factor for flux f_A^{Φ}, calculated as function of intermediate aperture area S_{co} from 0 to 2 cm^2, for a set of realistic cavity wall reflectivities from 92% to 99%. As expected, high attenuation values are obtained at small window aperture and at low wall reflectivity. In the first case less power is transferred from the first to the second cavity, whereas in the second case more power is lost as heat on the walls of the two cavities. To expand the dynamics of the attenuation factor, the area S_{co} is changed by using inserts with different aperture area, which are introduced in a slit between the two spheres (see next paragraphs). The values of f_A^{Φ} shown in Fig. 2 are restricted to a few hundreds. Higher values, in the order of thousands, are obtained by reducing the input window area S_{in}. A ray-tracing study on the fluxmeter has been carried out by using the TracePro code. The simulation has been applied to the original CAD project, that used by the manufacturer to realize the DCR prototype. Fig. 3 shows a typical optical simulation.

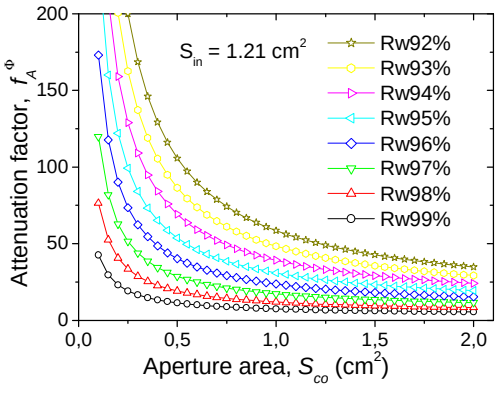

Fig. 2. Attenuation factor for flux f_A^{Φ}.

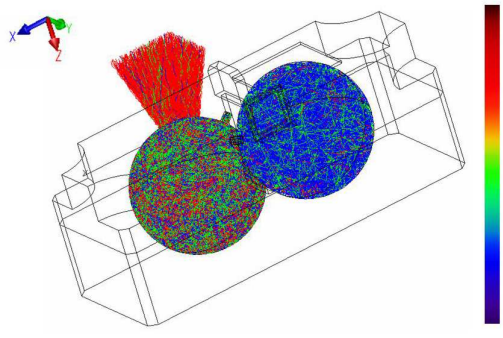

Fig. 3. Intensity of irradiation in the two cavities of the fluxmeter after a ray tracing study.

A simulated light beam, of known power, number of rays and angular distribution, enters the first cavity, having the concentration region (CR) exactly correspondent to the entrance aperture (win) of the radiometer. Part of light is lost back through (win), part of light is transferred to the second cavity. In fig. 3, at the stationary state, we distinguish the power content of each ray by its colour. Moreover, the distribution of colours in the two cavities allows to qualitatively estimate the irradiation intensity and distribution. It is evident the attenuation the light undergoes moving from the first to the second cavity, and the more uniformly distributed light intensity in the second cavity with respect to the first one. In this last cavity, moreover, is also visible a central region on the bottom, facing the input aperture, that is more illuminated as it corresponds to the area of first impact of the input beam. The ray-tracing model allows to analyze in detail the irradiation distribution into the cavities. It is evident that an additional integrating sphere assures a better distribution of light on the photodetector and then a less dependent response on the input beam geometry. We have analysed, for each cavity, six different portions of the wall. For each area we have calculated the incident power and the corresponding attenuation factor, normalized to the average value calculated for each sphere. The results are reported in Fig. 4. As can be seen, one decade smaller statistical variations are observable on the flux density in the second sphere with respect to the first one.

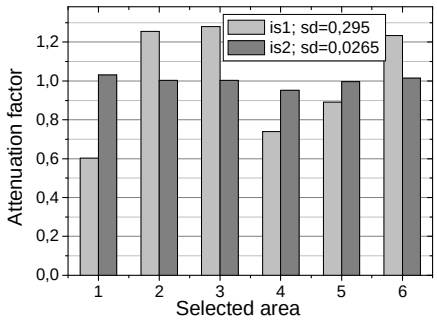

Fig. 4. Normalized average light intensity on six surface portions (4 cm^2 area) of the internal wall of each cavity (sd = standard deviation).

A uniform irradiation distribution into the second cavity is a prerequisite to obtain a constant response of the radiometer, in terms of attenuation factor, at constant power in input. The second aspect to investigate is the response of fluxmeter to the angular divergence of the beam into the first cavity at constant flux at input (see next paragraph).

THE FLUXMETER

Fig. 5 shows the general scheme of the radiometer, which includes all the accessories and instrumentations needed to thermoregulate the photodetector, to measure the photocurrent I_{ph}, and the spectrum of the radiation.

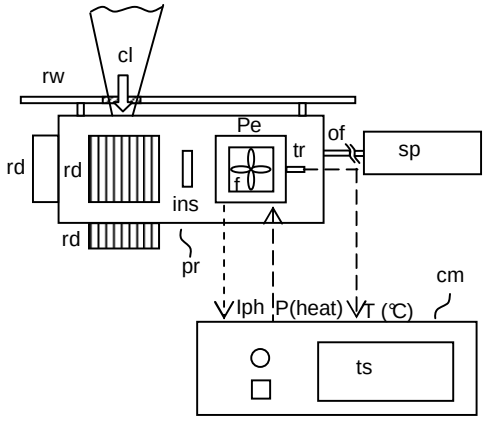

Figure 5. General scheme of the fluxmeter.

The control module (cm) provides the electric power P(heat) needed to drive the Peltier cooling system (Pe), cooled by the fan (f), and to control the temperature of the SP-HECO252 cell in the 5□-60 ℃ interval (typical operational temperature is 25℃). The temperature T (℃) of the photodetector is set out through the touchscreen (ts) on the (cm) and is measured by the thermistor (tr). The photocurrent of the cell is obtained by measuring the voltage drop on the 0.01 ohm shunt resistance (Rsh). The gauge head of fluxmeter (pr) was fabricated by working a prism of Aluminum, and is made of two sections joined at the horizontal plane. It can be protected on the front side by a reflective wall (rw) acting as a mirror and reducing the heating of accessories. The first cavity, the most involved in the heating process, is cooled by finned radiators (rd) placed on four walls of the prism.

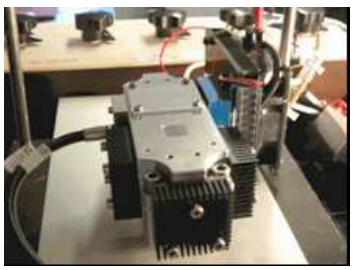

Fig. 6. Photo of the fluxmeter gauge sensor.

The insert (ins), whose aperture area can be changed between ten and hundred square millimeters, is introduced in the slit opened in the middle of the prism between the two cavities.The spectrograph (sp) is connected to the gauge head by an optical fiber (of), placed just in front of the detector. The complete fluxmeter was fabricated by ECOVIDE (Italy) [8]. A photo of the fluxmeter is shown in Fig. 6.

The fluxmeter was calibrated by the PASAN mod. 3B pulsed solar simulator. A Fresnel lens was used to concentrate the light of the simulator on a 1 cm^2 area. The calibration was carried out by measuring the photocurrent of a SunPower HECO 252 test cell used as reference (1.21 cm^2 area), the same used as photodetector in the fluxmeter, and then by measuring the photocurrent given by the fluxmeter. The input window (win) was (1.4x1.4 = 1.96 cm^2 area) was able to accept all the flux of the beam CR. This operation was repeated for different levels of light concentration and for different types of inserts. The experimental values of attenuation factor f_A^{Φ} have been compared to the theoretical data of the optical model and of the raytracing analysis. The comparison is better outlined by a log/log plotting and by a linear fitting of the data:

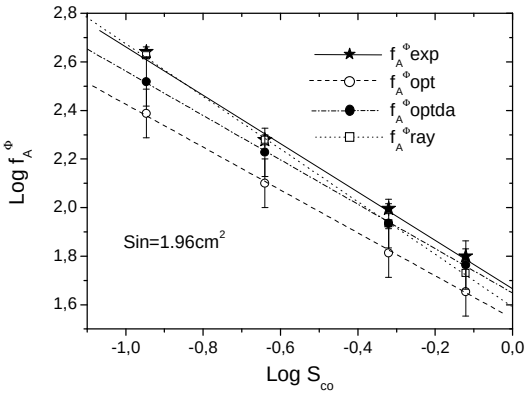

Fig. 7. Experimental (exp) and theoretical data of attenuation factor for flux f_A^{Φ}. Suffixes: opt = optical model; optda = optical model + dark area; ray = raytracing model.

$$\log f_A^{\Phi} = a + b \cdot \log S_{co} \qquad (4)$$

Fig. 7 shows the linear plots. The data from the ray-tracing model give the best matching with the experimental ones. The optical model has been artificially improved by adding 1 cm^2 of black area in each cavity to simulate the light absorption due to regions of the cavities difficult to model. In conclusion, the calibration measurements give for the attenuation factor the relationship:

$$\log f_A^{\Phi} = 1.66 - 1.01 \cdot \log S_{co} \qquad (5)$$

We have analysed so far the fluxmeter at a fixed geometrical configuration of the beam and in absence of

baffles. A baffle, however, is necessary in the first cavity (see (b1) in Fig. 8a), when the input beam divergence is high enough that some radiation directly enters the second cavity from the input window. Similarly, two other baffles are necessary in the second cavity for hiding the photodetector and the optical fiber from light entering (is2) though (wco) (see(b2) and (b3) Fig. 8b).

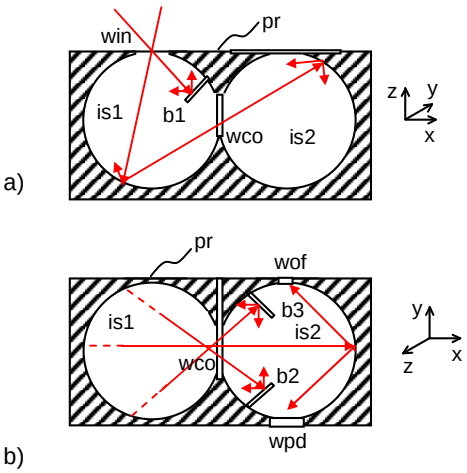

Fig. 8. Vertical (a) and horizontal (b) sections of the gauge sensor.

Now on we analyze by raytracing the response of fluxmeter at beams with different divergence at constant power in input, in presence or not of the three baffles. Fig. 9 shows, as expected, an average attenuation higher with baffles, due to the transfer of light from (is1) to (is2) limited by (b2) and (b3), which act as reflectors. Fig. 9 shows also two strong oscillations of f_A^{Φ}: one increase at ~50° in presence of baffles, due to the reflecting effect of (b1) respect to input radiation from (win); the other at ~40° in absence of baffles, due to the direct input of light from (win) into (is2). Maximum oscillations of f_A^{Φ} are around 5%. These oscillations have been strongly reduced by modifying the internal configuration of the two cavities. In Fig. 10 we report only the final results, which show that the oscillations, lower than ~0.5%, have been reduced of one order of magnitude.

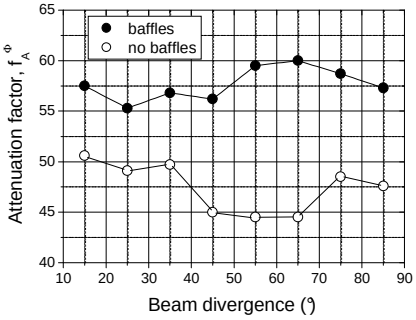

Fig. 9. Attenuation factor calculated as function of input beam divergence.

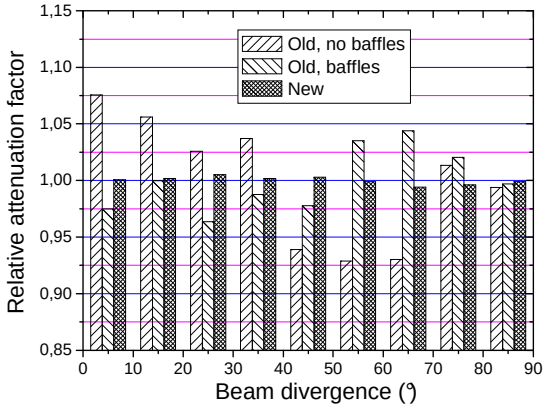

Fig. 10. Attenuation calculated by the ray-tracing method for the new version of fluxmeter [9].

CONCLUSIONS

We have described a fluxmeter for flux density measurements in solar concentrators, whose main characteristics are: the attenuation of radiation is allowed in a simple and precise way; flux density from few suns to thousands of suns can be measured (four decades of dynamic range); the response is fairly independent of the angular divergence of input beam; it is equipped with an external spectrometer for spectral measurements; measurements are carried out under stationary irradiation regime; the photodetector is thermoregulated for a constant sensitivity; easy to operate and portable.

REFERENCES

[1] A. Luque, G. Sala, J.C. Arboiro, T. Bruton, D. Cunningham and N. Mason. “Some results of the EUCLIDES photovoltaic concentrator prototype”. *Progress in Photovoltaics: Research and Applications 1997.* **5**, pp. 195-212.

[2] I. Antón, D. Pachón and G. Sala, “Characterization of Optical Collectors for Concentration Photovoltaic Applications”, *Progress in Photovoltaics: Research and Applications 2003.* **11**, pp. 387-405.

[3] A. Parretta, C. Privato, G. Nenna, A. Antonini, M. Stefancich, “Monitoring of concentrated radiation beam for photovoltaic and thermal solar energy conversion applications”, *Applied Optics* 2006. **45** pp. 7885-7897.

[4] A. Ferriere, and B. Rivoire, “Measurement of Concentrated Solar Radiation: The Asterix Calorimeter,” in Proc. 10th SolarPACES Int. Symposium on Solar Thermal Concentrating Technologies, Sydney, 8-10 March 2000, H. Kreetz, Ed. (ANU Australia), pp. 233-240.